

Ultrasonic Bonding for MEMS Sealing and Packaging

Jongbaeg Kim, Bongwon Jeong, Mu Chiao, and Liwei Lin

Abstract—The feasibility of ultrasonic bonding for hermetic microelectromechanical systems (MEMS) packaging has been demonstrated utilizing the solid phase vibration and welding process to bond two elements rapidly at low temperature. Two different approaches have been developed including lateral and vertical ultrasonic bonding setups with three sets of material bonding systems: In-to-Au, Al-to-Al, and plastics-to-plastics. The process utilizes purely mechanical vibration energy to enable low temperature bonding between similar or dissimilar materials without precleaning of the bonding surfaces. In these prototype demonstrations, the typical bonding process used tens of Watts at room temperature environment and the bonds were accomplished within seconds for bonding cavities with areas of a few mm². Preliminary tests show that packaged MEMS cavities can survive gross leakage tests by immersing the bonded chip into liquids. As such, ultrasonic bonding could potentially be broadly applied for hermetic MEMS sealing and packaging especially where temperature limitation is a critical issue. Ultrasonic polymeric bonding could be applied for capping polymer-based microfluidic chips. This paper describes the ultrasonic bonding and hermetic sealing processes as well as the characterizations of bonding tools and equipment setups.

Index Terms—Hermetic sealing, microelectromechanical devices, micromachining, packaging, ultrasonic bonding.

I. INTRODUCTION

ULTRASONIC energy has been used successfully in various applications such as nondestructive evaluations for mechanical properties of solid materials [1], ultrasonography in medical imaging systems [2], power sources for ultrasonic-based motors [3], [4], and manufacturing processes including cleaning, metalizing, soldering, machining, and bonding [5]–[7]. Ultrasonic bonding, firstly developed in mid-1960s, produces welds with high joint strength and good electric/thermal conductivity, and has found its applications where fast bonding and low bonding temperature are required. In macroscale, ultrasonic bonding technique is used for mechanical joining and fastening of metals and polymer structures, and is especially effective when used for joining of very thin sheets of various materials. It also enables the bonding of materials that could not be joined easily by standard technology.

Manuscript received November 30, 2007; revised October 07, 2008. First published March 16, 2009; current version published May 28, 2009. This work was supported by Seoul R&BD Program under Grant GR070039 and Grant 11032. This work was recommended for publication by Associate Editor A. Chiou upon evaluation of the reviewers comments.

J. Kim and B. Jeong are with the School of Mechanical Engineering, Yonsei University, Seoul 120-749, Korea (e-mail: kimjb@yonsei.ac.kr).

M. Chiao is with the Department of Mechanical Engineering, University of British Columbia, Vancouver, BC, V6T 1Z4 Canada.

L. Lin is with the Berkeley Sensor and Actuator Center, University of California, Berkeley, CA 94720 USA.

Color versions of one or more of the figures in this paper are available online at <http://ieeexplore.ieee.org>.

Digital Object Identifier 10.1109/TADVP.2008.2009927

For example, dissimilar materials such as ceramic and metal plates can be joined together with this method [8].

Ultrasonic bonding has been used to achieve reliable electrical connections such as wire bonding and flip-chip assembly [9]–[11]. Wire bonding is one of the dominant chip-connection technologies in microscale devices [12]. It is cost-effective since the process can be done without the needs for very expensive instruments, and the processing time is rather short. Although a number of new bonding techniques were developed since the wire bonding technology was introduced, semi-conductor industries still strongly depend on it. Ultrasonic-enhanced flip-chip assembly, usually referred as thermosonic flip-chip bonding, is another emerging chip-connection technology, which utilizes ultrasonic energy along with the thermal energy for chip-connections. Ultrasonic energy applied during the bonding process generates acoustic softening effect leading to local plastic deformation, which eventually lowers the processing temperature and pressure compared with the conventional flip-chip process [13]. Although it requires precise control on processing parameters such as co-planarity to produce fine packaging [14], thermosonic flip-chip bonding is quite attractive since the process is done under low temperature and pressure in reduced time.

Rapid bonding and low temperature processing are main advantages of the ultrasonic bonding technique. Even though the surface temperature may rise up to 200 °C–300 °C due to the friction of two contacting metal surfaces [15], the heating process is localized and bonding time is very short. For example, it has been demonstrated that ultrasonic bonding can be performed even under the liquid nitrogen environment [16]. It shows that the bonding process does not require high temperature and it can be suitable for microelectromechanical systems (MEMS) packaging where low temperature must be maintained. In addition to low temperature process, it has other merits compared to other bonding methods. For example, it does not require prebonding preparation or post-bonding treatments, consumes very little energy and can be easily automated.

Proper design of ultrasonic horn and die holder, the intensity and direction of ultrasonic field, compressive load and bonding time are some of the common parameters affecting the bonding efficiency and quality [17], [18], while achieving hermeticity is for reliability and durability of micro devices is specific for MEMS [19]–[21]. Since the surface tension force acts strongly in the microscale, a very small amount of liquid inside the package may cause stiction of internal structures, therefore resulting in unrecoverable malfunctioning of devices [22]. Ultrasonic hermetic bonding could be a good choice for MEMS packaging to enhance the reliability of MEMS by preventing the liquid ingress.

This paper describes ultrasonic bonding techniques for MEMS hermetic encapsulations applications. Unlike the thermosonic flip-chip bonding process for electrical connections, the chip substrates were not preheated and the hermetic sealing process was performed at room temperature. Two sets of different materials were investigated as bonding layers, including In/Au and Al/Al. Furthermore, the proper range of bonding parameters are developed for successful sealing for both sets of bonding materials.

II. ULTRASONIC BONDING PRINCIPLE AND EQUIPMENT SETUP

Ultrasonic bonding is a solid phase welding process which is primarily accomplished by softening one or both of the weldments with ultrasonic energy or heat [23]. As explained in the mechanism of softening metals by Langenecker [24], ultrasonic energy absorbed into metal causes multiplication and migration of dislocations resulting in an increase of density and mobility of dislocations and a reduction of shear stress necessary for plastic deformation of metals. Consequently, easy slip mechanism occurs within the crystal lattice of metal and yield strength is reduced [25]. The resulting shear metal flow under compressive load pushes most of contaminants, such as oxides and dirt, aside into debris areas and exposes essentially clean areas. Direct contact and diffusion at the newly generated metal surfaces result in bond formation. The heat generated by scrubbing two contacting surfaces during the bonding process could play a significant role for the diffusion at the contacting surfaces. It is known that increasing ultrasonic power and bonding time generally enhances the diffusion process, for better intermetallic phase and stronger bonds [26].

The essential components for the bonding test are the ultrasonic transducer, power control unit, and die holder [27]. In this bonding test, an ultrasonic transducer and horn system for wire bonding and flip chip die bonding were used with a power control unit (Uthe Tech. Inc, 21PT and 50 G). The power control unit maintains constant voltage for different types of die holders and generates ~ 60 -kHz mechanical vibration through the transducer. When the friction load is applied to the die holder, the frequency is reduced slightly but the power control unit is designed to operate within a specified range of impedance such that the frictional load caused by the two contacting dies during the bonding process did not generate significant frequency shift. The ultrasonic frequency of ~ 60 kHz used in this bonding test is generally applied for Al and Au wire bonding for electrical connection. Because the vibratory displacement at the end of a horn usually decreases as the frequency increases, transducers with lower frequencies than 60 kHz are typically used in macroscale ultrasonic welding applications and higher frequencies are adopted for smaller feature bonding such as fine pitch wire and flip chip bonding. We concluded that about 60–75 kHz is a moderate frequency range for MEMS scale bonding and packaging applications, where the vibratory displacement is in the order of several microns as characterized experimentally in the following experimental session.

Fig. 1 shows the equipment design where the ultrasonic actuator is powered by a control unit and the vibration amplitude is measured by a laser interferometer. The transducer and

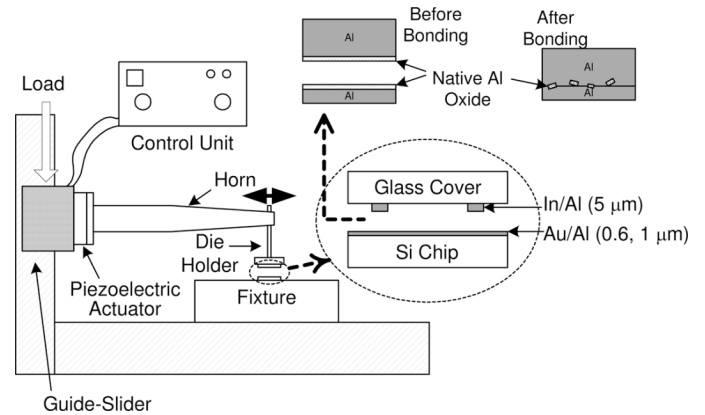


Fig. 1. Schematic diagram of the lateral bonding equipment setup and the nature of Al-to-Al ultrasonic bonding.

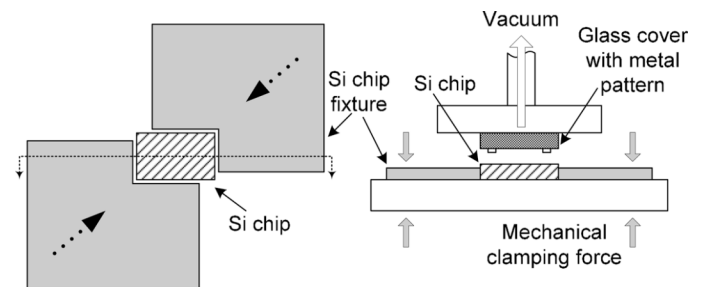


Fig. 2. Die holding mechanism and fixture on the bonding equipment: (left) top view of the Si die fixture, (right) side view of the whole mechanism.

horn unit is mounted on a slider which can move on a vertical guide so that the height of the horn can be adjusted for different specimen thickness and the required pressure on the die can be applied effectively. Load, vibration amplitude (or ultrasonic power), and actuating time are three important parameters in ultrasonic bonding. In this setup, load is applied vertically to generate pressure between two chips, and both time and power are controlled by the control unit. The actuator is composed of a piezoelectric transducer to generate high frequency vibration and a horn to amplify it. The horn has length of 69.6 mm with converging diameter from 13.0 to 5.3 mm at the tip. The die holder has a length of 32 and diameter of 2.9 mm for the shank portion and the collet is 1.8 mm thick with diameter of 13 mm. A die holder for mounting a topside glass cover is attached longitudinally at the end of the horn. The bottom Si chip is attached to a fixture.

The rigidity of the die clamping device on the work stage is important to effectively generate the relative motion between the fixed bottom chip and moving glass cover. As shown in Fig. 2, the glass cover is held on the die holder (tool) by vacuum force and the Si chip is tightly clamped on the work stage by the holding fixture made of high stiffness tungsten carbide. This die fixture designed here gives very high rigidity in lateral direction, constrains the die at one fixed position and may hold different sizes of chips easily. Fig. 3 is a picture of the whole equipment setup including the ultrasonic actuator for vibrating a top die and the stage to hold bottom die. The stage is made of Al which has a good thermal conductivity to enhance the transfer of frictional heat generated from the contacting surfaces of the glass

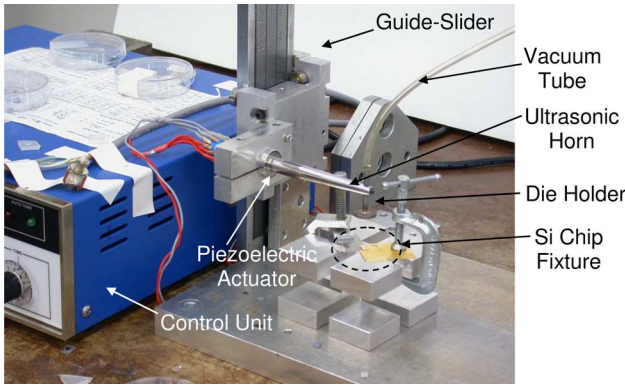


Fig. 3. Picture of the lateral bonding equipment setup.

cover and Si chips. It is noted that most of the frictional heat is propagated and dissipated by conduction across the Si substrate and the stage. Furthermore, it is important to have a good heat sink as a stage to minimize the temperature increase in the Si substrate. Top surface finishing of the stage during the machining for the stage manufacturing is another factor to consider because smoother stage surface can reduce the thermal contact resistance significantly.

To find out the optimal die holder position for effective ultrasonic power transmission, the displacement of glass chip was measured using laser interferometer. We divided the whole length of the shank into nine equal parts and conducted *in situ* measurement of the collet displacement as shown in Fig. 4(a) for each of the nine positions through which the vibration energy is transferred to the die holder and therefore to the top side glass cover. Fig. 4(a) shows that the pick-to-valley displacement ranges from $+0.75 \mu\text{m}$ to $-0.75 \mu\text{m}$ and the maximum power transmission occurred when the holder is attached to the horn at the sixth position. This measurement matches with the finite element analysis result in Fig. 4(b). It clearly shows that the sixth position corresponds to the anti-nodal point where the vibration input should be applied to get large displacement at the collet. The frequency of this vibration mode is 60.4 kHz which falls into the operating frequency range.

The vertical mode of ultrasonic energy transfer was also conducted. Fig. 5 shows the setup of bonding equipment, which is a typical configuration for ultrasonic plastic joining applications. In this setup, the mechanical energy from the horn is directly transferred to the glass and Si chips without passing through the die holder. So the ultrasonic energy is efficiently used for bonding and no characterization of die holder is necessary. However, when the bonded materials are brittle as in this experiment of Si and glass bonding, they are easily broken on the rigid fixture under vertical vibration. For this reason, the rubber pad was inserted under the Si chip. In addition to the protection of bonding chips, rubber pad gives two more functions; it holds the chips to maintain the alignment, and allows self-planarization of two contacting surfaces. Even though the rubber may partially insulate the ultrasonic from fully coupling into the interface as it is also moving, the usage of rubber pad is important considering uniform contact of Si and glass chips is one of the key conditions that should be satisfied for the successful hermetic sealing. Dummy Si die was used to minimize

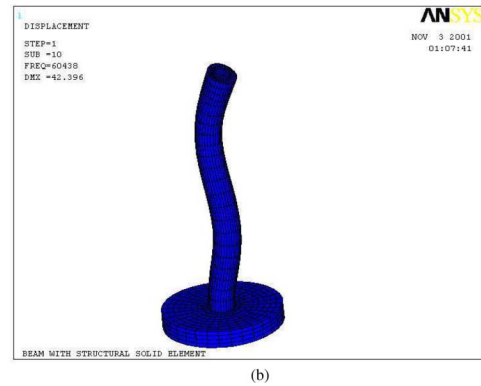
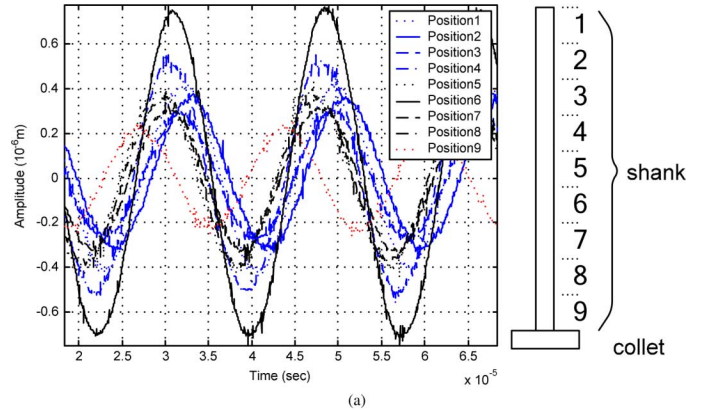


Fig. 4. (a) *In situ* measurement of the amplitude of vibration for loaded cases under various actuating positions along the die holder. (b) FE modal analysis of die holder vibration.

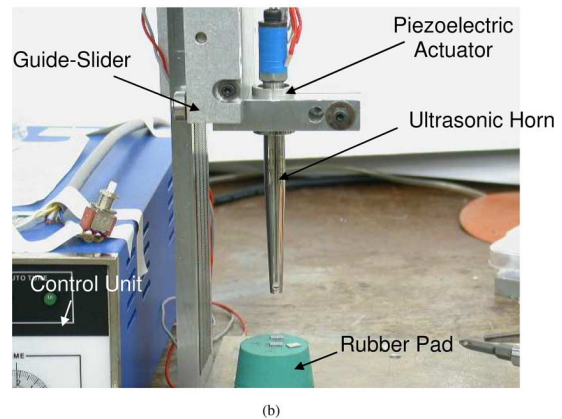
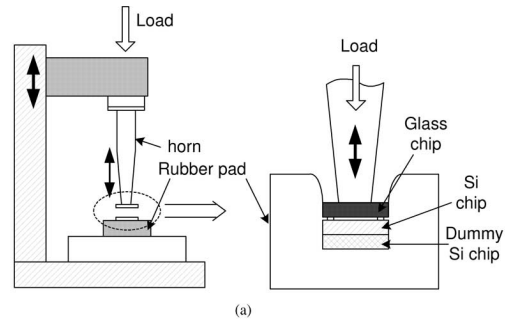


Fig. 5. Equipment setup of vertical ultrasonic bonding. (a) Schematic diagram of vertical setup and rubber pad for uniform contact. (b) Picture of vertical setup.

the possible bending of test chips and to protect test chips from sticking to the rubber surface due to the increased temperature.

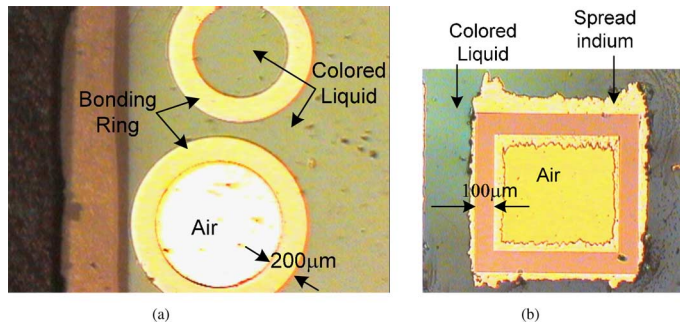


Fig. 6. (a) Ultrasonic In/Au bonding under the leakage test showing hermetically sealed (below) and failed (top) bonding rings. (b) Ultrasonic In/Au bonding result showing that bonding pattern has spread out due to the excessive bonding power and time.

III. SAMPLE PREPARATION, BONDING RESULTS, AND DISCUSSIONS

A. Lateral and Metallic Bonding

The test samples are prepared as two different sets. The first set is composed of 6000 Å Au-coated Si chips and 5-μm-thick In-patterned glass chips. The second set is 1-μm-thick Al-coated Si chips and 5-μm-thick Al-patterned glass chips. All chips are cut into 4 mm × 6 mm size for both glass and Si substrates. A 3000 Å chromium layer was deposited first before Al for the second set. Furthermore, a chromium layer between Si and Al is recommended not only because of the good adhesion characteristics of Si/Cr and Cr/Al, but also because Si is soluble in Al up to a few percent. Without the Cr layer, there may be the possibility of defects such as Al spiking in Si under Al to cause both electrical and mechanical reliability problems.

All bonding layers were deposited by metal evaporation. Deposited metals by evaporation or sputtering also form polycrystalline structures and native defects such as dislocation that may assist the bonding process [24]. Grain boundaries and defects in evaporated or sputtered metals for electrical interconnection in IC devices can cause problems such as high resistivity or electromigration. In ultrasonic bonding for MEMS packaging, it is expected that those defects enable the decrease of yield strength of metals and facilitate the plastic flow of metal under the propagation of ultrasonic energy.

Fig. 6 shows the hermeticity testing result of Au-coated Si and In-patterned glass by immersing the bonded system into colored liquid. Highly volatile and wettable IPA (Isopropyl Alcohol) is used as the liquid at room temperature and atmospheric pressure. The liquid does not penetrate into the bonding-ring (the bottom one) that has outside diameter of 1200 μm and width of 200 μm as the preliminary demonstration that hermetic bonding is accomplished. For comparison, the top bonding-ring failed the gross leakage as shown. Fig. 6(b) is presented to demonstrate the importance of ultrasonic bonding parameters. The square-shaped bonding ring here shows characteristics of hermetic seal, but the bonding solder spreads out significantly when the excessive ultrasonic energy is applied. According to the finite element analysis, the temperature at the bonding interface may rise up to more than 200 °C during the bonding process and this is high enough to melt low melting point metal such as In (156 °C).

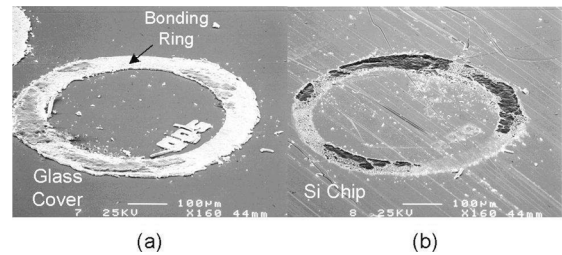


Fig. 7. SEM microphotos of In to Au bonding after the bond is forcefully broken: (a) glass cover and (b) Si chip.

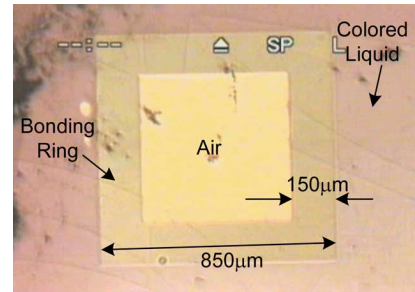


Fig. 8. Hermetically sealed aluminum-to-aluminum bond by ultrasonic bonding.

However, this figure shows the negative effects of excessive ultrasonic bonding power or time as spreading of In occurs during the bonding process. It is also possible that the spreading may be from the excessive pressure during the bonding process since In is very soft material. With the vertical setup in Fig. 5, In/Au bonding was successfully demonstrated but the pattern spilled out more frequently during the repeated experiments.

The bonded system is then forcefully broken and examined under SEM with the glass cover in Fig. 7(a) and Si substrate in Fig. 7(b). It is observed that a great portion of Au layer that was originally on the Si substrate has been torn off and is now attached to the glass cover. Similar phenomena are observed for Al-to-Al bonding shown in Figs. 8 and 9. No liquid leakage can be identified inside the square shape bonding-ring in Fig. 8 as hermetic seal is accomplished. The square bonding-ring is 850 μm in size (outside width) and has a ring width of 150 μm. The majority of the Al patterns, which were originally deposited on the glass cover in Fig. 9(a) have transferred to the Si chip in Fig. 9(b). Fig. 9(c) and (d) are optical microphotos of another set of bonded Al sample after the bond is forcefully broken. In contrast to the In/Au bonding system, spreading of Al was not observed regardless of the amount of applied ultrasonic power or time used in the experiments.

The bonding results described above for both In/Au and Al/Al bonding systems are all performed with the lateral transducer and horn setup. If either the bonding power or time is reduced, it was observed that the bonding is formed only at the outer perimeter of the bonding rings and these chips failed in the hermeticity tests. This observation implies that ultrasonic welding starts around the perimeter and propagates to the inner area of the bonding rings. As the bonding power and time are increased, the number of dies that were successfully bonded and passed the preliminary hermeticity tests by immersing the bonded chip

TABLE I
BONDING PARAMETERS USED IN THE EXPERIMENTS

Parameters	In/Au	Al/Al	Polymeric bonding (cellulose acetate)
Power supply output	20~25 Watts	30~50 Watts	20 Watts
Bonding time	0.8~1.8 sec	2.5~5.0 sec	2.0 sec
Pressure	9.20~15.4 MPa	20.8~40.1 MPa	1.03~2.58 MPa
Vibration amplitude	0.8~1.5 μm	0.8~1.5 μm	N/A
Total bonding area on one chip	1.59~2.12 mm^2	1.59~2.12 mm^2	1.90 mm^2

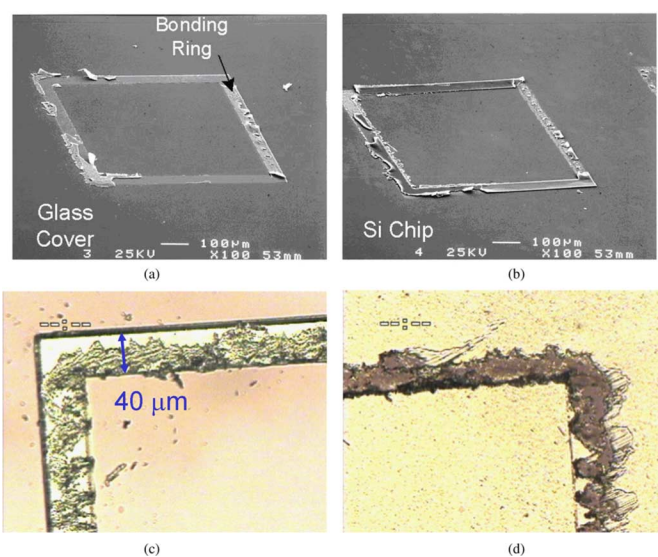


Fig. 9. Al-to-Al bonding after the bond is forcefully broken. The result of first pair is shown in (a) cover and (b) Si substrate. It is observed that Al on the glass is transferred to the Si substrate. The result of second pair is shown in (c) glass and (d) Si substrate.

into liquids for leakage tests. Different bonding periods ranging from 0.1 to 10 s were applied for the same bonding ring shape and area. When the bonding time is smaller than 5 s for the Al bonding system, the number of successfully bonded patterns (there were six bonding rings on one die) increased with time. No obvious correlation can be drawn between the bonding ring features and bonding time when the ultrasonic actuator was activated for more than 5 s. Furthermore, minimum bonding time for good yield is increased when the bonding area is increased. For the In to Au bonding system, the overall bonding time required to achieve good yield was shorter (mostly less than 1.8 s). All parameters used in the experiments are summarized in Table I using the lateral setup. The range of values for power, time and pressure show upper and lower bounds with which at least more than one pattern out of six on the same chip were sealed hermetically. These results were obtained with the specific amplifier and die holder as described and optimal operation conditions will require new characterizations if new amplifier, die holder or material bonding systems are used.

B. Vertical and Polymeric Bonding

For the vertical bonding setup, polymeric materials are the major bonding systems in our studies as it is rather difficult to have good polymer bonding results at room temperature environment. Previously, localized resistive heating has been demonstrated for packaging for polymer-based MEMS [28]. Another good example for possible application is the sealing of microfluidic channels fabricated by polymeric materials. For example, injection molding, casting or hot embossing can easily duplicate micro polymeric that do not have top caps [29] and ultrasonic bonding and sealing could be applicable. While no hermetic enclosure can be created using polymers, polymeric microchannels are typically bonded and sealed by gluing, heating or laser welding [30]. For some polymers with low surface energy, such as PDMS, plasma oxidation of polymer surface enhances adhesion to wide variety of materials, and has been adopted to seal microfluidic channels [31]. In this section, ultrasonic bonding technique is applied to thermoplastic polymer material for localized heating and bonding.

The mechanism of ultrasonic bonding of polymer is slightly different from that of ultrasonic metallic bonding systems presented in the preceding sections. In polymer bonding processes, frictional heat energy induced by ultrasonic energy can easily reach the required activation energy for bonding of polymers. Fig. 10 shows demonstration results of using cellulose acetate, one of the biocompatible, thermoplastic polymers. Two and three 500- μm -thick cellulose acetate substrates are stacked up and bonded by ultrasonic energy. For three layer bonding, the middle layer has a drilled hole with diameter of 1 mm to form a cavity after the bonding process is completed. As shown in Fig. 10(a), the vibration direction of the ultrasonic bonding tool is perpendicular to the planes of stacked cellulose acetate layers and accordingly, the dynamic load is applied to the surface of cellulose acetate. This additional load deforms the area underneath the bonding tool locally as a ring shape shown in Fig. 10(b). Fig. 10(c) is the side view of three layer bonding result where a pair of tweezers are holding the middle layer of the bonded cellulose acetate.

To avoid the ring-shape formation that absorbed the majority of the energy from the vertical bonding setup, the lateral bonding setup can be used. Fig. 11(a) shows a plastic bonding example with the lateral bonding setup. The polymer has a

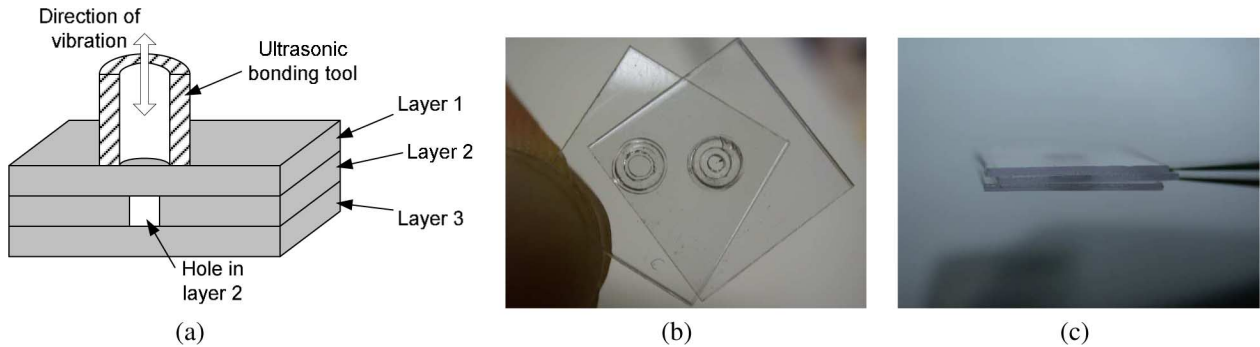


Fig. 10. (a) Experimental setup of the vertical ultrasonic bonding of three layers of cellulose acetate. (b) Optical photo of the two-layer polymer bonding result. The outer and inner diameters of the ultrasonic amplifier are 1.8 and 0.85 mm, respectively, as reflected and shown on the polymer substrates. At the center of the right side bonding ring, there is a 0.5-mm-diameter drilled hole on one side of two bonded layers. (c) Side view of three bonded layers.

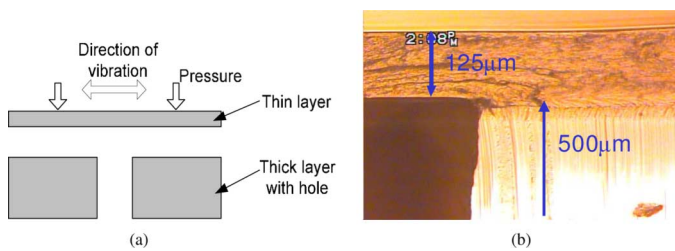


Fig. 11. Ultrasonic bonding of cellulose acetate layers using the lateral bonding setup. (a) A hole drilled in the base substrate is to be enclosed by the top thin cellulose acetate layer. (b) Cross sectional view of the bonding result.

drilled hole of 1 mm in diameter and a 125- μm -thick cellulose acetate is used to cover it. In Fig. 11(b), the bonded sample is cut through the drilled hole by a razor to show the cross sectional view. Similar to the metal bonding cases as described in the previous session, ultrasonic power, bonding time and load are the three key parameters to be controlled for successful polymer bonding. The right amount of load is especially important for these soft polymeric materials and extra energy may deform the polymer enough to narrow or clog the microfluidic channel. Nevertheless, our preliminary bonding results show good sealing under leakage tests using water as the working fluid. In Table I are shown parameters used for successful cellulose acetate bonding in our test. Further investigations on the optimal processing conditions of various polymeric material systems and geometries will be necessary while the basic operation principles have been demonstrated in this paper.

IV. CONCLUSION

Ultrasonic bonding for hermetic sealing of MEMS sealing and packaging using several different material systems as bonding layers has been demonstrated. Unlike the conventional macro-scale ultrasonic welding or wire bonding for microelectronics, bonding layers used in this work are thin film metals or polymer materials for MEMS packaging and sealing applications. Ultrasonic power, load and operation time are three control parameters to be characterized to achieve hermetic sealing for MEMS application. In addition to these variables (power, pressure and time), flatness of two bonding surfaces and intimate contact are also important parameters

for successful bonding results. To achieve hermetic sealing, precision setup of bonding system and fixture design is critical. Even though the ultrasonic bonding process generally does not require precleaning of bonding interface or posttreatment, big particles or dusts must be avoided to achieve good contact of two bonding surfaces. Two different bonding equipment setups have been successfully used in experiments and it was concluded that the lateral vibration setup gives better bonding results for MEMS packaging and sealing applications while vertical vibration setup can cause local energy concentration and will be better applicable for specific bonding and sealing applications. With proper wafer holder design, these ultrasonic bonding techniques could be extended to wafer level packaging while keeping the low temperature at the bonding interface and substrate.

REFERENCES

- [1] R. E. Green Jr., *Treatise on Materials Science and Technology vol. 3: Ultrasonic Investigation of Mechanical Property*. New York: Academic, 1973, pp. 1–2.
- [2] J. I. DiStasio, *Ultrasonics as a medical diagnostic tool*. Park Ridge, NJ: Noyes, 1980, pp. 1–23.
- [3] S. Ueha and Y. Tomiyaka, *Ultrasonic Motors: Theory and Applications*. New York: Oxford Univ. Press, 1993, pp. 197–230.
- [4] T. Sashida and T. Kenjo, *An Introduction to Ultrasonic Motors*. New York: Oxford Univ. Press, 1993, pp. 17–23.
- [5] A. Puskar, *The Use of High-Intensity Ultrasonics*. New York: Elsevier, 1982, pp. 43–55.
- [6] S. H. Yeo and L. K. Tan, “Effects of ultrasonic vibrations in micro electro-discharge machining of microholes,” *J. Micromechan. Microeng.*, vol. 9, pp. 345–352, 1999.
- [7] X. Sun, T. Masuzawa, and M. Fujino, “Micro ultrasonic machining and its applications in MEMS,” *Sensors Actuators A*, vol. 57, pp. 159–164, 1996.
- [8] N. Okamura and Y. Watanabe, “Ultrasonic joining of Si_3N_4 plates at 19 kHz using Al, Cu and Ni plates as insert metal,” *Jpn. J. Appl. Phys.*, vol. 38, no. 10, pt. 1, pp. 6166–6169, Oct. 1999.
- [9] J. Tsujino, “Review of ultrasonic welding of metal and plastic materials,” *J. Acoust. Soc. Jpn.*, vol. 45, no. 5, pp. 409–415, May 1989.
- [10] T. McLaren, S. Y. Kang, W. Zhang, D. Hellman, T. H. Ju, and Y. C. Lee, “Thermosonic flip-chip bonding for an 8*8 VCSEL array,” in *Proc. 45th Electron. Compon. Technol. Conf.*, Las Vegas, NV, May 21–24, 1995, pp. 393–400.
- [11] J. Tsujino, H. Yoshihara, T. Sano, and S. Ihara, “High-frequency ultrasonic wire bonding systems,” *Ultrasonic*, vol. 38, pp. 77–80, 2000.
- [12] R. Tummala, E. J. Rymaszewski, and A. Klopfenstein, *Microelectronics Packaging Handbook Part II: Semiconductor Packaging*, 2nd ed. London, U.K.: Chapman & Hall, 1997, pp. 186–187.
- [13] S. Y. Kang, P. M. Williams, T. S. McLaren, and Y. C. Lee, “Studies of thermosonic bonding for flip-chip assembly,” *Materials Chemistry Phys.*, vol. 42, pp. 31–37, 1995.

- [14] Q. Tan, B. Schaible, L. J. Bond, and Y. C. Lee, "Thermosonic flip-chip bonding system with a self-planarization feature using polymer," *IEEE Trans. Adv. Packag.*, vol. 22, no. 3, pp. 468–475, Aug. 1999.
- [15] J. Tsujino, T. Ueoka, Y. Asada, S. Taniguchi, and Y. Iwamura, "Measurement of the temperature rise at the welding surface of different metal specimens joined by a 15 kHz ultrasonic butt welding system," *Jpn. J. Appl. Phys.*, vol. 37, no. 5B, pt. 1, pp. 2996–3000, May 1998.
- [16] G. G. Harman and K. O. Leedy, "An experimental model of the micro-electronic ultrasonic wire bonding mechanism," in *Proc. 10th IEEE Annu. Conf. Reliabil. Phys.*, NY, 1972, pp. 49–56.
- [17] M. Hizukuri, N. Watanabe, and T. Asano, "Dynamic strain and chip damage during ultrasonic flip chip bonding," *Jpn. J. Appl. Phys.*, vol. 40, pp. 3044–3048, 2001.
- [18] K. Suga, E. Ohdaira, N. Masuzawa, and M. Ide, "Relationship between horn pressure and welding time in ultrasonic welding of plastic pipes using torsional vibration," *Jpn. J. Appl. Phys.*, vol. 38, pp. 3302–3306, May 1999.
- [19] Y. Cheng, L. Lin, and K. Najafi, "A hermetic glass-silicon package formed using localized aluminum/silicon-glass bonding," *J. Microelectromech. Syst.*, vol. 10, no. 3, pp. 392–399, Sept. 2000.
- [20] Y. Cheng, W. T. Hsu, K. Najafi, C. T. Nguyen, and L. Lin, "Vacuum packaging technology using localized aluminum/silicon-to glass bonding," *IEEE/ASME J. Microelectromech. Syst.*, vol. 11, no. 5, pp. 556–565, Oct. 2002.
- [21] M. Chiao and L. Lin, "Device-level hermetic packaging of microresonators by RTP aluminum-to-nitride bonding," *IEEE/ASME J. Microelectromech. Syst.*, vol. 15, no. 3, pp. 515–522, Jun. 2006.
- [22] M. R. Houston, R. Maboudian, and R. T. Howe, "Ammonium fluoride anti-stiction treatments for polysilicon microstructures," in *Proc. 8th Int. Conf. Solid-State Sensors Actuators Eurosensors IX*, Jun. 1995, pp. 210–213.
- [23] G. G. Harman and J. Albers, "The ultrasonic welding mechanism as applied to aluminum- and gold-wire bonding in microelectronics," *IEEE Trans. Parts, Hybrids Packag.*, vol. PHP-13, no. 4, pp. 406–412, Dec. 1977.
- [24] B. Langenecker, "Effects of ultrasound on deformation characteristics of metals," *IEEE Trans. Sonics Ultrasonics*, vol. SU-13, no. 1, pp. 1–8, 1966.
- [25] R. Tummala, *Fundamentals of Microsystems Packaging*, 1st ed. New York: McGraw-Hill, 2001, pp. 346–353.
- [26] L. Levine, "The ultrasonic wedge bonding mechanism: Two theories converge," *Proc. SPIE—Int. Soc. Opt. Eng.*, vol. 2649, pp. 242–246, 1995.
- [27] J. Kim, M. Chiao, and L. Lin, "Ultrasonic Bonding of In/Au and Al/Al for Hermetic Sealing of MEMS Packaging," in *15th Annu. IEEE Int. MicroElectro Mechan. Syst. Conf.*, 2002, pp. 415–418.
- [28] Y. C. Su and L. Lin, "Localized bonding processes for assembly and packaging of polymeric MEMS," *IEEE Trans. Adv. Packag.*, vol. 28, no. 4, pp. 635–642, Nov. 2005.
- [29] F. Sammoura, J. J. Kang, Y. M. Heo, T. S. Jung, and L. Lin, "Polymeric microneedle fabrication using a micro injection molding technique," *Microsyst. Technol. J.*, vol. 13, pp. 517–522, 2007.
- [30] H. Becker and C. Gartner, "Polymer microfabrication methods for microfluidic analytical applications," *Electrophoresis*, vol. 21, no. 1, pp. 12–26, 2000.
- [31] D. C. Duffy, J. C. McDonald, O. J. A. Schueller, and G. M. Whitesides, "Rapid prototyping of microfluidic systems in poly(dimethylsiloxane)," *Analytical Chem.*, vol. 70, no. 23, pp. 4974–4984, 1998.

Authors' photograph and biographies not available at the time of publication.